

Modeling the Spread of COVID-19 Using a Novel Threat Surface

TED G. LEWIS¹ AND
WALEED I. AL MANNAI²

Abstract: Classical models of epidemic spreading based on making contact within a susceptible population assume a constant infection rate and uniform mixing. As such, they cannot account for surges and waves which have been observed in practice. This paper describes the spreading as a byproduct of interacting with a threat surface $S(x, y)$ containing susceptible populations at location (x, y) in a 2D grid. The discretized grid acts as a transmission vector for COVID-19 and may explain why COVID-19 spreading exhibits surges rather than obey a smooth logistics curve. Furthermore, the strong correlation between infection cases and population indicates that population and distribution of population over a 2D area may explain most of why infection cases surge and waves form. It is impossible to obtain an accurate prediction of the extent of spreading without taking public sentiment, spatial separation, and size of populations into account. The best predictor of the ultimate spread of COVID-19 considers population as well as infection rate.

We find that a terrain-based model is capable of modeling surges and waves of epidemics in most countries and regions where public sentiment is mild. In other cases where public sentiment is opposed to social distancing, wearing masks, and generally against public health policy, a two or three phase approach is necessary, whereby each phase is fit with different parameters, suggesting that public sentiment has a bigger influence on contagion spreading than population. We validate our results through simulation of outbreaks in a diverse set of countries and regions, e.g., a county in the US, Bahrain, Israel, United Kingdom, Germany, South Korea, and Italy.

Keywords: COVID-19, simulation and modeling of epidemics, threat surface, public sentiment, non-uniform mixing, infectious disease, size of epidemic.

1.0 MOTIVATION

Classical models grounded in SIR models (Susceptible—Infected—Recovered/Removed) like the logistics growth model and the Kermack-McKendrick model, assume constant infection rate, uniform mixing, and constant removal rate. None of these factors exist in the real world, whereby populations exhibit radically uneven mixing, variable infection and recovery rates, and variable population sizes. For example, COVID-19 exhibits a spreading pattern where-

by future daily infections are based on previous daily infections, changing reproduction number R_0 and changing recovery rate.

Spreading depends on public sentiment and public health policy as much as the virus itself. Public health policy in the form of social distancing, wearing a mask, and hand-washing hygiene is often at odds with public sentiment which may be politically or socially opposed (or accepting) of official public health policy. In other words, human behavior is responsible for spreading in addition to population size. Spatial isolation is the most effective way to limit spreading, regardless of population size [3, 4, 5, 6, 7, 8].

This paper proposes a novel alternative approach to modeling epidemic spreading. Instead of a constant infection rate and one monolithic susceptible population we introduce a threat surface $S(x, y)$ defined over a 2D area with number of susceptible individuals and variable infection rate at each coordinate (x, y) on the surface. In other words, we propose to break a geographical region into discrete parts—cells—and solve for number of infections in each cell and then sum them for the entire region. Spreading occurs locally, i.e., through contact with 8 adjacent cells: NW, N, NE, W, E, SW, S, SE. The magnitude of infection rate at each coordinate (x, y) depends on the number of infected individuals at a previous time, called the *delay*. The number of infected cases at each coordinate depends on the number during the previous time step (days), spreading rate, and variable infection rate. Infection rate is computed using a feedback mechanisms whereby previous infections at time $(t-\text{delay})$ influence infection rate at time t .

Essentially, this model breaks the Kermack-McKendrick SIR model into discretized local models over a surface $S(x, y)$. At each cell (x, y) , a modified SIR model is applied using the local susceptible population, local infected cases, and a variable infection rate. The number of infected cases is then the sum over all local cells, which is plotted as a curve versus time. As it turns out, this approach exposes waves in the infection curve caused by non-uniformity of susceptible population and variations in the infection rate.

Classical models assume a uniformly distributed population with the same levels of immunity or susceptibility to infection, and a relatively immobile population. On the contrary, the modern world violates all of these conditions: populations are clustered, people of different age and economic conditions have different susceptibilities to disease, public opinion as to the dangers of a contagion shift over time, and modern people are extremely mobile thus making frequent contacts with one another. This makes modeling COVID-19 extremely complicated and multi-faceted.

Of particular interest in this paper is the incidence of subsequent waves of COVID-19 infection that have been observed nearly in every region of the world. After an initial rise that is fairly predictable using standard models, there follows a brief period of decline, and then one or more subsequent surges, often exceeding the initial peak infection. Waves are observed in COVID-19 and were observed in the Spanish Flu pandemic of 1918. What causes these surges and how can we predict them? Our hypothesis is that this observed effect is a combination of public sentiment and local population clusters.

There are many explanations for these surges or waves, which defy mathematical modeling by traditional models [1]. For example, the *SIS*—*susceptible-infected-susceptible* model is completely inadequate to explain these waves. The traditional Kermack-McKendrick (KM) model, and more recently, network-based models, cannot represent these recurrent outbreaks because they assume that infections rise and fall one time, only. Models based on smoothly rising curves cannot approximate reality that is far messier, involving humans and governments. In reality, epidemics such as COVID-19 go through one or more wave-like behaviors whereby the daily infections rise and fall many times, largely due to a variety of factors such as public sentiment and population densities.

2.0 MODEL FORMULATION

The crux of our model is a variable infection rate that depends on how many people are infected at location (x, y) . Thus, infection rate increases/decreases depending on the variation in population terrain. We assume all information needed to predict the state of a contagion is contained in a *threat surface* $S(x, y)$ defined as a function or data at each coordinate (x, y) in two dimensions. If the geometry of this surface is similar to

the real world and the dynamics describes what happens when individuals come into contact with the surface, then spreading will occur as observed regardless of non-uniform mixing. We use model similitude to explain the spread of COVID-19.³

We develop an entirely new model based on a parameterized differential-difference equation. Our model has four parameters to be determined by fitting a curve produced by simulation with observed measurements (counts or cases):

- N: Mean number of susceptible people in a cell.
- α : Spreading rate from coordinate-to-adjacent-coordinate in $S(x, y)$
- β_0 : Mean infection rate
- t_0 : Mean time delay.

Let $M(t)$ be the cumulative number of new cases on day t . Then the Kermack-McKendrick value for each coordinate $S(x, y)$ is given by the solution to:

$$\frac{dM(t)}{dt} = (\beta_0 - \beta(t - t_0))[M(t)(N - M(t))] \quad (1)$$

Or in discrete time:

$$\Delta M(t) = (\beta_0 - \beta(t - t_0))[M(t)(N - M(t))] \quad (2)$$

Where,

$\frac{dM(t)}{dt}$ is a model of the number of daily infections and $M(t)$ is the discrete analog representing daily change in total number infected cases. $\Delta M(t)/M(t)$ is a suitable measure of public sentiment either pro or con public health recommendations like social distancing. Thus, $\beta(t-t_0)$ is the variable infection rate that depends on the number of daily infections in the past—with lag time of t_0 . For mild waves and surges, we use:

$$\beta(t - t_0) = \beta_0 - \frac{\Delta M(t-t_0)}{M(t-t_0)} > 0 \quad (3)$$

Infection rate varies with the time rate of daily cases reported t_0 days in the past. That is, future infection rate lags by t_0 days, approximating human behavior—the rate declines when the number of infections in the past rise; and increases when the number of infections in the past declines. We argue people get overconfident when the rate of infection declines, and fearful when the rate climbs. This contributes to minor waves of infections in the spreading curve, but it is only one influence. A more suitable model that addresses extreme surges and waves is presented in section 3.2.

2.1 The Threat Surface/Terrain Model

A terrain or threat surface is a 3D “map” of a geographical region where COVID-19 spreading is due to the presence of a susceptible population that “fuels” spreading. We know that spreading increases in intensity and speed where the population is large, and less spreading occurs where the population is sparse. There are multiple reasons for this, such as crowding and more frequent contact.

We define $S(x, y)$ as a 3D Excel spreadsheet with n rows and m columns in two dimensions, and population in the third dimension. Each cell is created by overlaying the spreadsheet on top of a map of the region to be studied and assigned the population number at that cell/geographical location. For example, in Figure 1, the population ranges from 1 to 40,000 for a total of over 513,000 people within Monterey county, California. Most of the county is empty, while small regions are highly populated. Salinas, for example, has over 150,000 people, while Monterey has approximately 45,000.

Spreading rate α determines the speed of the advancing COVID-19 virus and must be estimated by trial-and-error to scale to the dimensions of $S(x, y)$. An infected cell at (x, y) transmits the infection to adjacent neighbors with probability α . Higher values mean more rapid transmission. This is separate from the person-to-person rate, $\beta(t-t_0)$ that determines number of susceptible people that contract the disease upon spreading.

Simulating the spread of COVID-19 is simply a process of planting a seed (first infection) at some location (x, y) , and allowing it to spread from cell to adjacent cell with probability α . The number of individuals infected at each time step, t , is governed by solving equation (2) and (3) at each t . This produces a curve for $M(t)$ and daily infections, $\Delta M(t)$ versus t as shown in Figure 2.

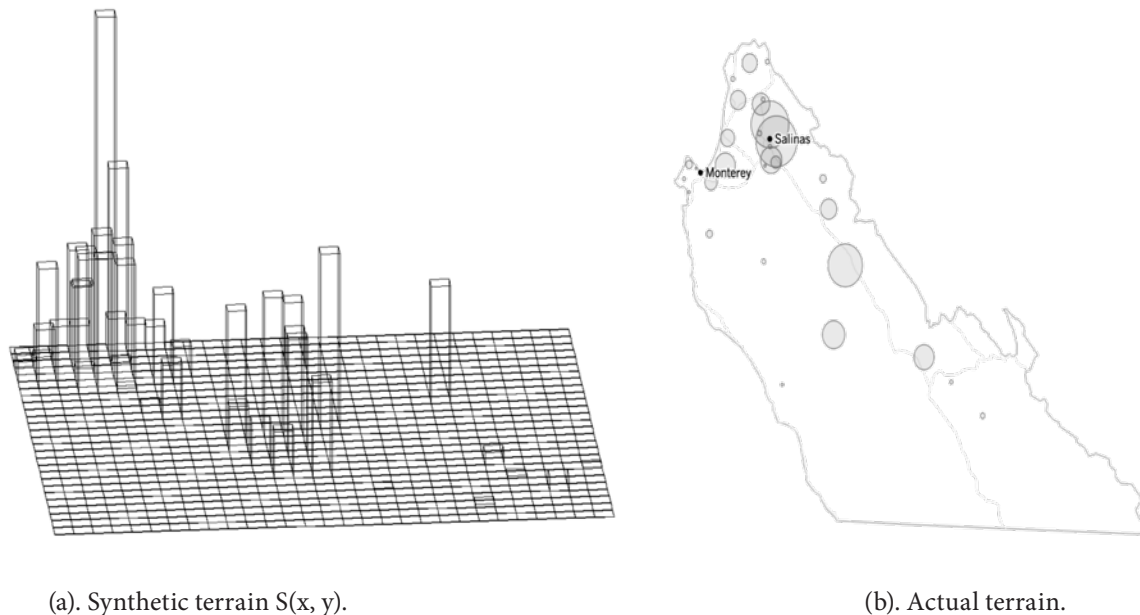


Figure 1. (a). Terrain model of Monterey County, California with $n = 29$ rows and $m = 27$ columns representing the approximate population at each cell. (b). Actual terrain of Monterey County with COVID-19 outbreaks is indicated by circular regions.

2.2 PandemiX

PandemiX is a computer program developed by the authors that takes parameters for (2) and terrain model $S(x, y)$ as input and produces infection curves for $M(t)$ and daily infections, $\Delta M(t)$ versus t , as outputs, see Figure 2. The animated spreading propagates from input coordinates (x_0, y_0) , and eventually reaches the entire terrain.

The algorithm is very simple, and depends on $S(x, y)$ and four parameters $N, \alpha, \beta_0,$ and t_0 .

Algorithm 1. PandemiX Simulation

1. Plant an infection at location (x_0, y_0) in $S(x, y)$.
2. Repeat until no further infections ($t \gg 0$):
 - a. For every (x, y) in S :
 - b. For each neighbor of (x, y) let $r =$ random number in $(0, 1)$.
 - i. If $(r \leq \alpha)$ calculate:
 1. $\beta(t-t_0)$, and apply to ...
 2. ... $\Delta M(t)$ and $M(t)$ at (x, y) .
 - c. Total over all (x, y) to get number of cases at time t .

- d. Increment t.
- 3. End

The 8 nearest neighbors are the adjacent cells NW, N, NE, W, E, SW, S, SE for each cell shown in Figure 3. At each time step and location (x, y), each of the 8 adjacent cells are infected with probability α . This is repeated for $t = 1, 2, 3, \dots$ until no further infections occur.

Each cell has a susceptible population as shown graphically in Figure 1. Each time an infected cell is visited, it increases the adjacent infected cells by an amount given by equation (2) and (3). Infected cells exhibit diminishing returns, because $[N-M(t)]$ steadily decreases until reaching zero and further infections stop. Placement of the initial infection is very important, however, in most cases the exact location of the initial infection is not known. Accordingly, we default to a relatively unpopulated area as initial infection coordinates (x_0, y_0) .

This model conspicuously does not account for mobility or the impact of human movement. Mobility is considered in a network-based model by the authors published earlier [1]. Essentially, flows into and out of connected regions can be modeled as epidemics on a network surface. It is beyond the scope of this paper.

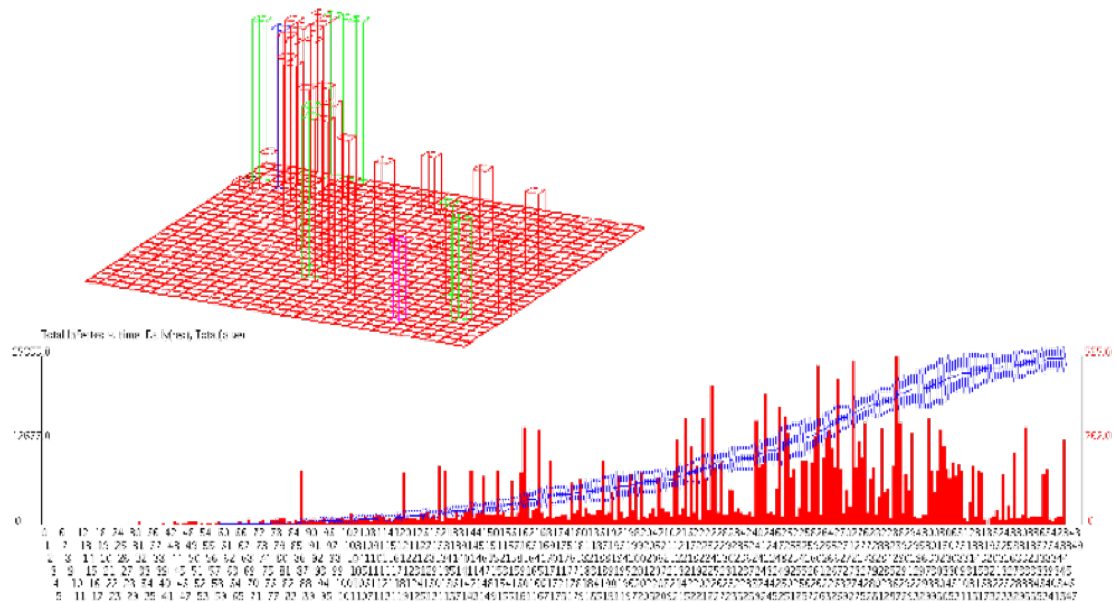


Figure 2. PandemiX displays the averages of numerous trials, and the animated terrain as the infection spreads. Red bars are the average daily infections; the central blue line is the average total infections, and the other blue lines are upper and lower bounds obtained by also computing the sampling error assuming a two-tailed confidence level of 97.5%.

NW	N	NE
W	x, y	E
SW	S	SE

Figure 3. Nearest neighbors with number of susceptible individuals $[N-M(t)]$, are infected with probability α each time the cell is visited. The number of cases rise over time according to equation (2).

3.0 APPLYING MODEL SIMILITUDE

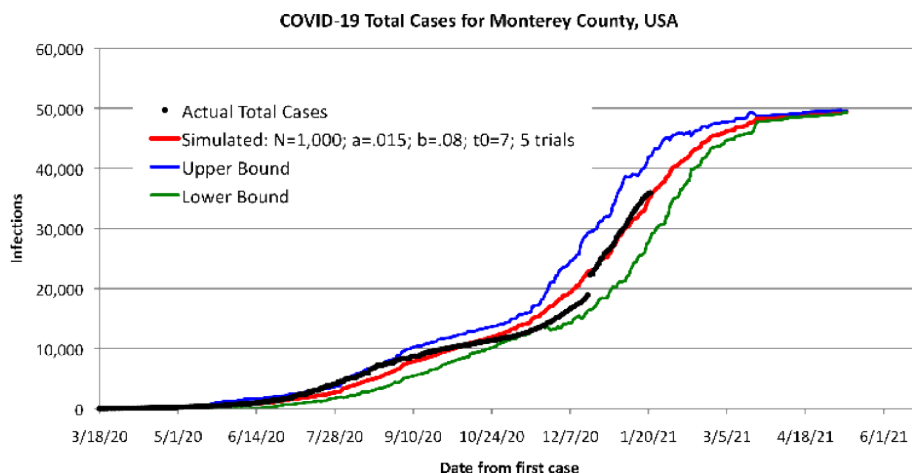
Figure 4 shows the results of applying the model to COVID-19 data for Monterey county, USA and Bahrain. Monterey county has over 513,000 residents and over 30,000 infected cases as of January 10, 2021. Bahrain has over 1.7 million residents with over 90,000 infected cases. Numerous simulations were required to find the best fit of $\Delta M(t)$ and $M(t)$ to empirical data, with the final result for Monterey county:

- N: 1,000
- α : 0.015 (Speed)
- β_0 : 0.08 (virality)
- t_0 : 7 (delay)

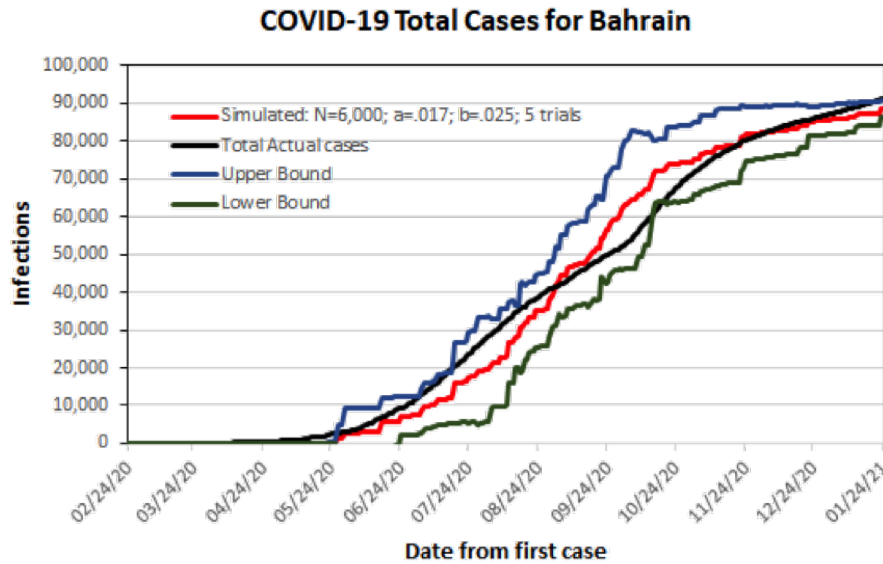
Five trials were averaged to obtain the red curve in Figure 4, along with an error of plus-or-minus blue and green lines. The red line is a very good fit to the actual recorded cases (black dotted line).

The results show an initial slow rise in COVID-19 followed by a rapid rise, then a second slowing followed by a second surge in cases. The model predicts a third decline in cases after the second surge, with the epidemic predicted to peak at roughly 50,000 cases by June 2021.

Subsequent simulations of other regions of the world give similar results. Table 1 summarizes them and shows that parameters differ for different parts of the world and different population sizes. Interestingly, nearly all simulations showed the best results for a time delay of 5-7 days. The largest difference is in N, which varies widely, but is somewhat correlated with total population of the country or region. In all cases, the infection curve is more accurate for the terrain model than KM or KM-derived models based on logistic growth.



(a). Monterey county, USA with over 500,00 population.



(b). Bahrain with over 1.7 million population.

Figure 4. Actual and simulated data for number of infections versus time for two different regions of the world. The actual data falls within the error bounds of the simulated data. Monterey data predicts future infections, as the number of infections decline.

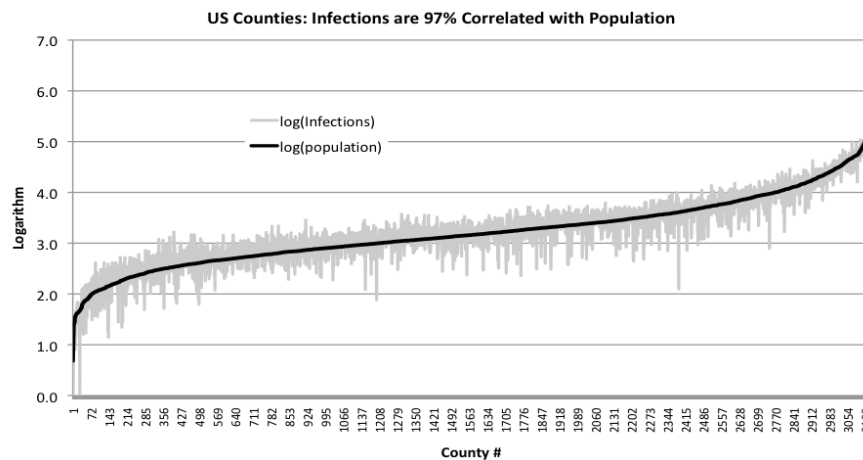


Figure 5. Infections and population are strongly correlated (0.97) as shown by the number of infection cases in the counties of the US as of 1/3/21.

Table I. Simulation parameters for various terrains throughout the world.

Region	#trials	N	α	β_0	t_0
Monterey	5	1,000	.015	.08	7
Bahrain	5	6,000	.017	.025	7
UK	5	1,000,000	.010	.017	20
S. Korea	5	25,000	.012	.018	5
Israel	5	150,000	.009	.060	5

3.1 An Oscillation Model

Villalobos-Arias [2] propose a wave model of an epidemic containing surges by overlaying multiple logistics curves. The model fits the COVID-19 epidemic very well but does not reveal underlying causes or enable forecasting of future infections. Indeed, epidemics within epidemics fit logistic curves as long as the end of one surge and the beginning of another can be detected in the data. This amounts to identifying oscillations in the time series while maintaining a constant infection rate. It assumes a constant infection rate, which may not hold, especially when human nature is involved.

We assume a varying infection rate that depends on public sentiment and public health policy. In particular, sentiment increases risk taking when the rate of infection declines and the reverse when the rate of infection increases. This, and variations in the terrain, creates oscillations in the daily time series. It is our considered opinion that population generally plays a bigger role in surges than public sentiment. When all 3141 counties in the USA were analyzed versus population, the observed correlation with population was very strong, see Figure 5. Both size of infection and population obeyed a power law and the two are correlated.

Surges and waves are a direct result of public sentiment (minor effect) and spatial separation of populations, and size of population. It is impossible to obtain an accurate prediction of the extent of spreading without taking public sentiment and spatial separation of populations into account. And, when public sentiment becomes extreme, as it has in some countries, the simple terrain model breaks down and a piecemeal model is required.

3.2 Extreme Waves

COVID-19 spread slowly in Germany until the summer of 2020, when anti-mask and anti-social-distancing protests broke out across the country. On August 29, 38,000 protesters gathered in Berlin to demonstrate against wearing masks, social distancing, and closing businesses. The massive protest continued through the Christmas holidays. As a result, a second wave, many times larger than the first under lockdown conditions, surged. Figure 6 shows the dramatic results.

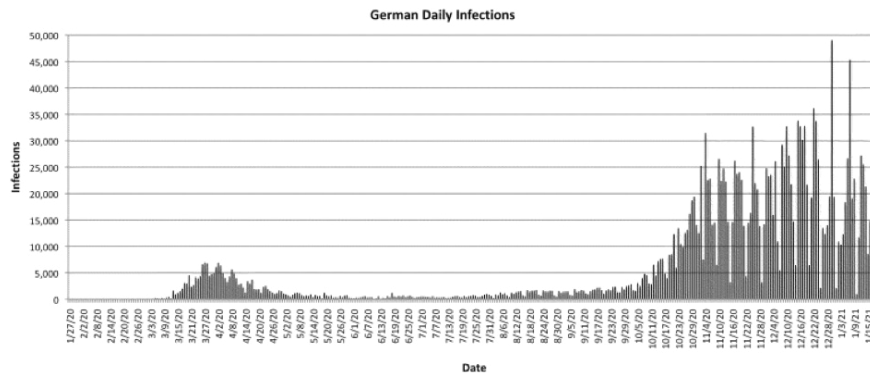
Our model does not allow sufficient feedback to adjust infection rate beta to match the rapid rise of the pandemic in Germany. Instead, a “two epidemics” model is required: one model of each mega-surge in infections. The parameters for both waves are given in Table 2 along with results for other regions with more than one major wave. In the case of South Korea, note the difference between the one-wave simulation and a three-wave simulation: the infection rate of the three-wave simulation straddles the one-wave infection rate. This suggests shifts in public sentiment directly affects the number of infection cases.

4.0 DISCUSSION

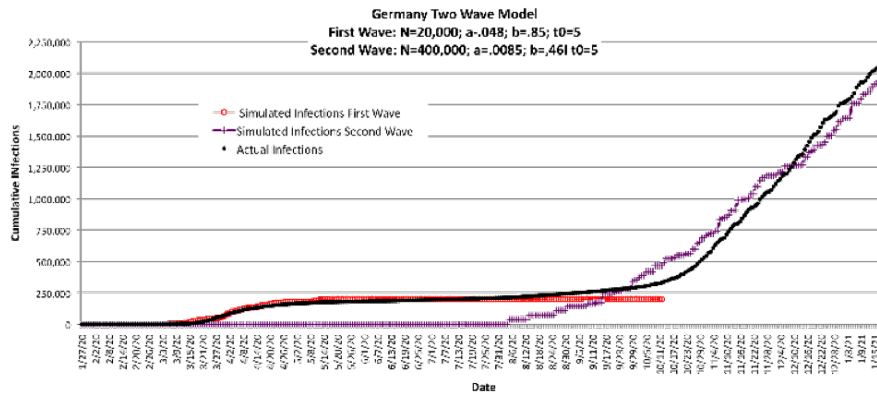
Using a population terrain as a means of epidemic spreading is a new idea in mathematical modeling of epidemics. It appears to provide deeper understanding of the spreading dynamics. However, it is not the complete answer. It has several weaknesses:

- The method lacks predictive power. The number of infections going forward in time are based on the time delay and therefore are only accurate for t_0 days ahead.
- Simulations are noisy. We had to average over 5 trials to obtain reasonable results. Even so, the confidence interval was quite large. Averaging in more trials tends to smooth out the curves too much.
- Our results depend on high fidelity terrains which are difficult to obtain. We used very course-grained population counts due to the time and effort needed to build high resolution models.

- Terrains are even more difficult to obtain for large countries like the US, India, and China. Our results have been verified for relatively small regions and may not hold for large regions.



(a). Two waves are apparent in Germany.



(b). The dual wave model treats each wave as independent “mini epidemics.”

Figure 6. (a). Daily infections peaked early in the COVID-19 pandemic, then took off again after August 29. (b). A two-wave model of the spread due to civil disobedience following the August 29 protests.

Table II. Simulation parameters for extreme waves.

Region	#trials	N	α	β_0	t_0
Germany Wave 1	5	20,000	.048	.85	5
German Wave 2	5	400,000	.0085	.461	5
Italy Wave 1	5	60,000	.015	2.0	5
Italy Wave 2	5	400,000	.015	.0003	5
S. Korea Wave 1	5	5,000	.085	.0938	5
S. Korea Wave 2	5	15,000	.015	.026	5
S. Korea Wave 3	5	25,000	.015	.00025	5

NOTES

- 1 Ted G. Lewis is an author, speaker, and consultant with expertise in applied complexity theory, homeland security, infrastructure systems, and early-stage startup strategies. He has served in both government, industry, and academe over a long career, including, Executive Director and Professor of Computer Science, Center for Homeland Defense and Security, Naval Postgraduate School; Senior Vice President of Eastman Kodak, President and CEO of DaimlerChrysler Research and Technology, North America, Inc., and Professor of Computer Science at Oregon State University, Corvallis. In addition, he has served as the Editor-in-Chief of a number of periodicals: IEEE Computer Magazine, IEEE Software Magazine as a member of the IEEE Computer Society Board of Governors and is currently Advisory Board Member of ACM Ubiquity and *Cosmos + Taxis*. He has published more than 35 books, most recently *The Signal: A History of Signal Processing*, *Book of Extremes: The Complexity of Everyday Things*, *Bak's Sand Pile: Strategies for a Catastrophic World*; *Network Science: Theory and Practice*, and *Critical Infrastructure Protection in Homeland Security: Defending a Networked Nation*. Lewis has authored or co-authored numerous scholarly articles in cross-disciplinary journals such as *Cognitive Systems Research*, *Homeland Security Affairs Journal*, *Journal of Risk Finance*, *Journal of Information Warfare*, *IEEE Parallel & Distributed Technology*, *Communications of the ACM*, and *American Scientist*.
- 2 Waleed I. Al Mannai served for 37 years in the Bahrain Ministry of Defence, retiring as a colonel with extensive experience in military aviation and operations, and teaching. He received his PhD in Modeling, Virtual Environments, and Simulation from the Naval Postgraduate School (NPS); his MSc in Aeronautical Engineering, also from the NPS and his BSc in Aerospace Engineering from Northrop University. His areas of research interest include Modeling and Simulation, Critical Infrastructure Protection (CIP), network risk and data analysis, and managerial decision analysis.
- 3 Similitude is a concept applicable to the testing of engineering models. A model is said to have similitude with the real world if the two share geometric similarity, kinematic similarity and dynamic similarity. [https://en.wikipedia.org/wiki/Similitude_\(model\)](https://en.wikipedia.org/wiki/Similitude_(model))

REFERENCES

- Ted G. Lewis and Waleed I. Al Mannai. 2021. Predicting the Size and Duration of the COVID-19 Pandemic. *Frontiers in Applied Mathematics and Statistics Journal*, Volume 6, Article 611854, March.
- Villalobos-Arias and Mario-Alberto 2020. Using generalized logistics regression to forecast population infected by COVID-19, arXiv:2004.02406v1 [q-bio.PE] 6 Apr.
- Hellewell, J., et al. 2020. Feasibility of controlling COVID-19 outbreaks by isolation of cases and contacts. *The Lancet Global Health*.
- Abel, T. and D. Mcqueen. 2020. The COVID-19 pandemic calls for spatial distancing and social closeness: not for social distancing! *International Journal of Public Health*. 65.
- Lai, S., et al. 2020. Effect of non-pharmaceutical interventions to contain COVID-19 in China. *Nature* 585(7825): 10-413.
- Kraemer, M.U.G., et al. 2020. The effect of human mobility and control measures on the COVID-19 epidemic in China. *Science* 368(6490): 493.
- Flaxman, S. et al. 2020 Estimating the effects of non-pharmaceutical interventions on COVID-19 in Europe. *Nature* 584(7820): 257-261.
- Bertuzzo, E. et al. 2020. The geography of COVID-19 spread in Italy and implications for the relaxation of confinement measures. *Nature Communications*. 11(1): 4264.